

Influence of Multilayers on Structural, Morphological, Luminescence and Magnetic Properties of ZnO Thin Films

Ali Fatima A. and Suganthi Devadason

*Thin Film Laboratory, Department of Physics,
Karunya University, Coimbatore-641 114, India*

Abstract

Zinc oxide (ZnO) thin films were grown on glass substrates using sol-gel spin coating technique. The nanocrystalline thin film of ZnO with hexagonal (Wurtzite) structure were characterized by X-ray powder diffraction (XRD), scanning electron microscopy (SEM), X-ray photoelectron spectroscopy (XPS), photoluminescence (PL) spectroscopy and vibrating sample magnetometer (VSM). With increasing number of layers the intensity of XRD increases. The chemical composition and stoichiometry of the ZnO thin films were investigated through XPS. The XPS spectrum recorded on ZnO thin films reveal the presence of only Zn and O. Room-temperature photoluminescence spectrum from ZnO shows a near band edge (NBE) emission band peaked at around 383 nm and a broad deep-level emission (DLE) band at around 496 nm, respectively.

Keywords: XRD, Nanocrystalline, X-ray photoelectron spectroscopy, VSM, Near band edge emission.

Introduction

Zinc oxide transparent conducting oxide (TCO) films have extensive applications in various fields such as solar cells [1] optical waveguides [2] and gas sensors [3]; has caused great increase in research on zinc oxide thin films.. Zinc oxide thin films are highly used in optoelectronic devices over other materials. There are different methods to prepare zinc oxide, such as, RF/DC magnetron sputtering [4,5], MOCVD [6], ALD [7], spray pyrolysis [8,9], pulsed laser deposition [10] and sol gel.

The sol-gel process has distinct advantages over than other techniques due to excellent compositional control, homogeneity on the molecular level due to the

mixing of liquid precursors and lower crystallization temperature of different thickness. In the present study, ZnO thin films were prepared on glass substrate by the sol gel spin coating method using homogeneous and stable zinc acetate dehydrate, ethanol and Diethanolamine sol. The crystal orientation, optical absorption, luminescence properties and magnetic properties were investigated.

Experimental Procedure

Sample preparation and Characterization

Nano-crystalline zinc oxide films have been prepared by the sol gel process. The precursor solution was prepared using zinc acetate dehydrate ($\text{Zn}(\text{CH}_3\text{COO})_2 \cdot 2\text{H}_2\text{O}$) in a solution of ethanol and diethanolamine. The molar ratio of DEA to zinc acetate was 1.0 M. The resultant solution was stirred at 50°C for 1h to yield a clear and homogeneous solution. The solution was stored at room temperature for one day.

The glass substrates were cleaned thoroughly by soap solution, water, dilute HCl and HNO_3 and finally with deionized water with the help of an ultrasonic bath. The substrate was spin coated with the sol with a speed of 3000 rpm for 30s in air. Each coating on the substrate was first dried in air at 200°C for 60 s and then annealed at 450°C for one hour in air. This process of coating and subsequent heat treatment was repeated for 2,4,6,8 and 10 times to get different thickness thin films.

The structural properties were studied by X-Ray Diffractometer using Cu $K\alpha$ radiation operated at 40 Kv and 30 mA. The microstructures were also examined by Scanning Electron Microscope. Compositions were verified by XPS. The optical properties were determined from transmission measurement in the range of 300-1000 nm using UV- Vis-NIR spectrometer.

Results and Discussions

Structural properties

The ZnO thin films were characterized by XRD to confirm the crystalline phase of the films. Fig.1 (a-e) shows the representative XRD pattern of ZnO thin films synthesized at 450°C , film revealing wurtzite phase of ZnO. The sharp XRD peaks imply good crystallinity. All deposited ZnO films showed crystalline nature whereas with increase in the number of layers, crystalline nature of the deposited ZnO films became more defined and progressively more intense and sharp for films with up to eight layered depositions. For the ten layered film, peaks were well defined and sharp but slight reduction in intensity were observed. X-ray diffraction (XRD) revealed a strong influence of thickness on film surface topography. X-ray diffraction based structural characterization shows that the ZnO films have grown predominantly along the c-axis (002) direction where the angular position of the (002) peak varies slightly with increasing film thickness[11].As the thickness of the film increased, the crystalline nature of the film improved, which is also in agreement with Linhua Xu et al [12].

The values of lattice constants a and c for various layers calculated using equation (1) and the calculated values are given in Table 1. Comparing with the lattice constants for hexagonal ZnO crystal given in JCPDS standard data file $a = 3.2498 \text{ \AA}$

and $c = 5.2066 \text{ \AA}$ [17], it is seen that the calculated values are in good agreement with the standard values for ZnO wurtzite structure.

Table.1 Lattice constants

Lattice constant	2 layers	4 layers	6 layers	8 layers	10 layers
a (Å)	3.24197	3.25955	3.25981	3.25430	3.24716
c (Å)	5.20150	5.21898	5.21990	5.21110	5.20734

$$\frac{1}{d^2} = \frac{4}{3} \left(\frac{h^2 + hk + k^2}{a^2} \right) + \frac{l^2}{c^2} \text{----- (1)}$$

Where ‘d’ is the inter planar spacing and $h, k,$ and l are the Miller indices.

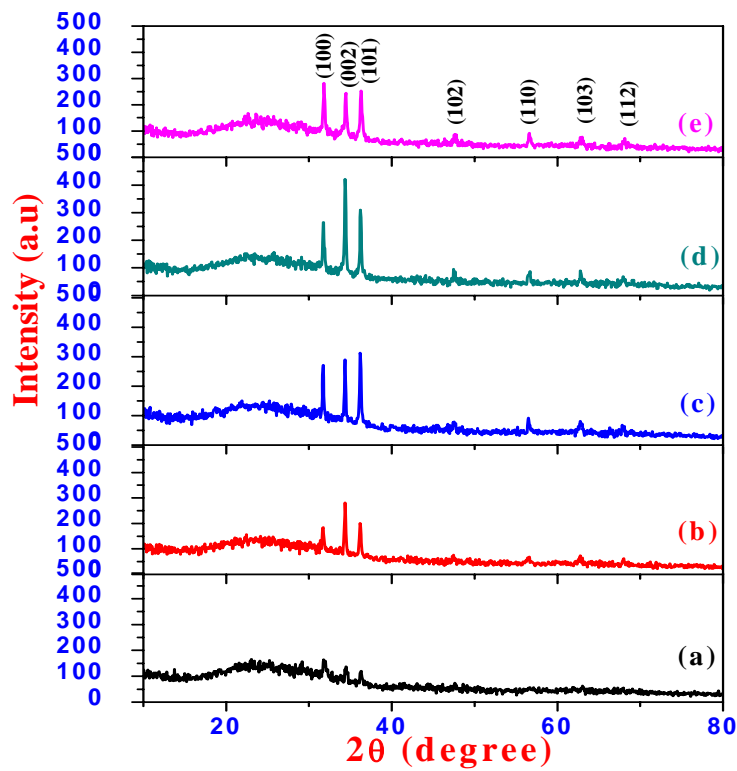


Figure 1(a-e). XRD spectrum of ZnO nanocrystals showing some prominent peaks

The surface morphology and micrographs of the ZnO thin films grown on glass substrate with different layers were observed by SEM. Fig. 2 (a-e) shows the surface

morphology of films with 2,4,6,8 and 10 layers. The surface morphologies of all the thin film samples are distinct. The surface morphology of the thin film grown upto 8 layers were more densely packed with some pits on it, while that grown with 10 layers slight agglomeration [13] appeared.

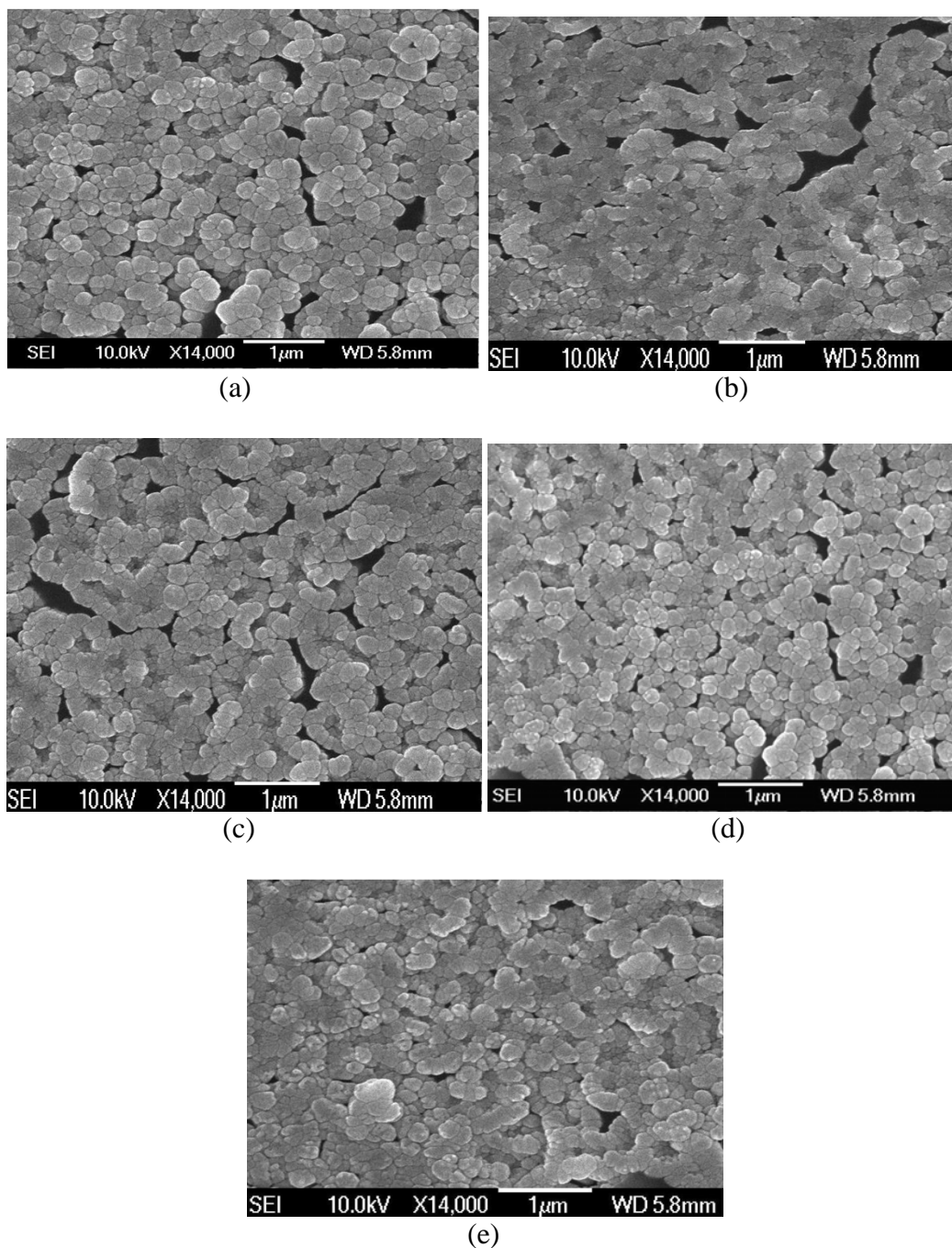


Figure 2. (a-e) SEM images were observed for 2,4,6,8 and 10 layers.

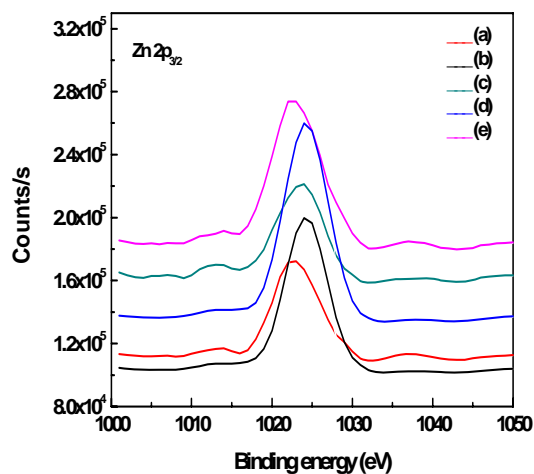


Figure 3: XPS close scan spectra ($\text{Zn } 2p_{3/2}$) of ZnO films with different thicknesses (a) 2 layer, (b) 4 layer, (c) 6 layer, (d) 8 layer and (e) 10 layer

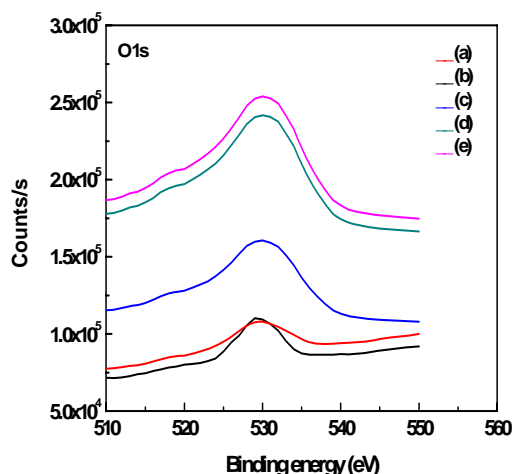


Figure 4: XPS close scan spectra ($\text{O } 1s$) of ZnO films with different thicknesses (a) 2 layer, (b) 4 layer, (c) 6 layer, (d) 8 layer and (e) 10 layer.

To find the stoichiometry of ZnO films, quantitative analysis should be carried out using the XPS analysis of $\text{Zn } 2p_{3/2}$ and $\text{O } 1s$ energy lines respectively, it is shown in Fig. 3. and Fig. 4. In the present study, the observed $\text{Zn } 2p_{3/2}$ peak located at 1022.58, 1024.16, 1023.61, 1024.16 and 1022.47 eV for the 2, 4, 6, 8 and 10 layers respectively, which is nearly the same as the standard value of 1021.8 eV. Also $\text{O } 1s$ peak positions are observed at 531.02, 529.96, 530.78, 531.05 and 531.12 eV for the 2, 4, 6, 8 and 10 respectively. It is very close to the standard value of 530.05 eV. The important observation is that the XPS peak intensities increase with the increasing thickness of the ZnO films. Observation of these $\text{Zn } 2p_{3/2}$ and $\text{O } 1s$ peaks confirm the

presence of these elements in the ZnO film studied here. The stoichiometry was found out from this peak, which gives the presence of Zn : O as 1.02 : 0.98.

Optical properties

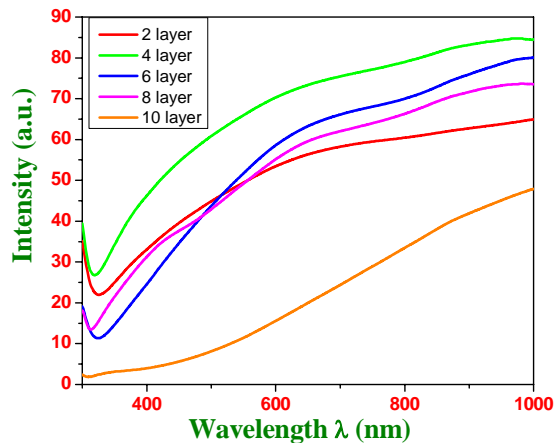


Figure 4 Optical transmission spectra of the ZnO multilayer thin films Measured at room temperature using UV-Vis -NIR spectrometer

Figure 4 shows the optical transmission spectra of the ZnO thin films with various layers measured at room temperature using UV-Vis-NIR spectrometer. All the films show 60-80% transmission in the visible region except for 10 layers. The band gap energy (E_g) of the multilayer thin film was calculated from the plot of $(\alpha h\nu)^2$ versus $h\nu$, where α is the optical absorption coefficient and $h\nu$ is the energy of the incident photon. Assuming a direct transition between valence and conduction bands, the energy band gap (E_g) was determined by from the expression

$$\alpha h\nu = K (h\nu - E_g)^{1/2} \quad (2)$$

where K is a constant. E_g is determined by extrapolating the straight line portion of the curve to $(\alpha h\nu)^2 = 0$. The absorption coefficient (α) of ZnO films was determined from transmittance measurements. Since envelope method is not valid in the strong absorption region, the calculation of the absorption coefficient (α) of the film in this region was calculated using the following expression

$$\alpha = \frac{\ln\left(\frac{1}{T}\right)}{t} \quad (3)$$

where T is the normalized transmittance and t is the film thickness.

Figure 5 shows $(\alpha h\nu)^2$ plots of the ZnO thin films as a function of photon energy. The band gap energies, obtained using the Fig. 5, of the multilayer thin films are 2.97, 3.03, 3.06, 3.13 and 3.03 eV for the ZnO thin films with 2,4,6,8 and 10 layers respectively. The bandgap energies obtained in this study for pure ZnO are lower than the bulk ZnO value of 3.37 eV. By increasing the number of layers of ZnO, the effective band gap energy of the multilayer thin films increased in this study as reported by others. [14].

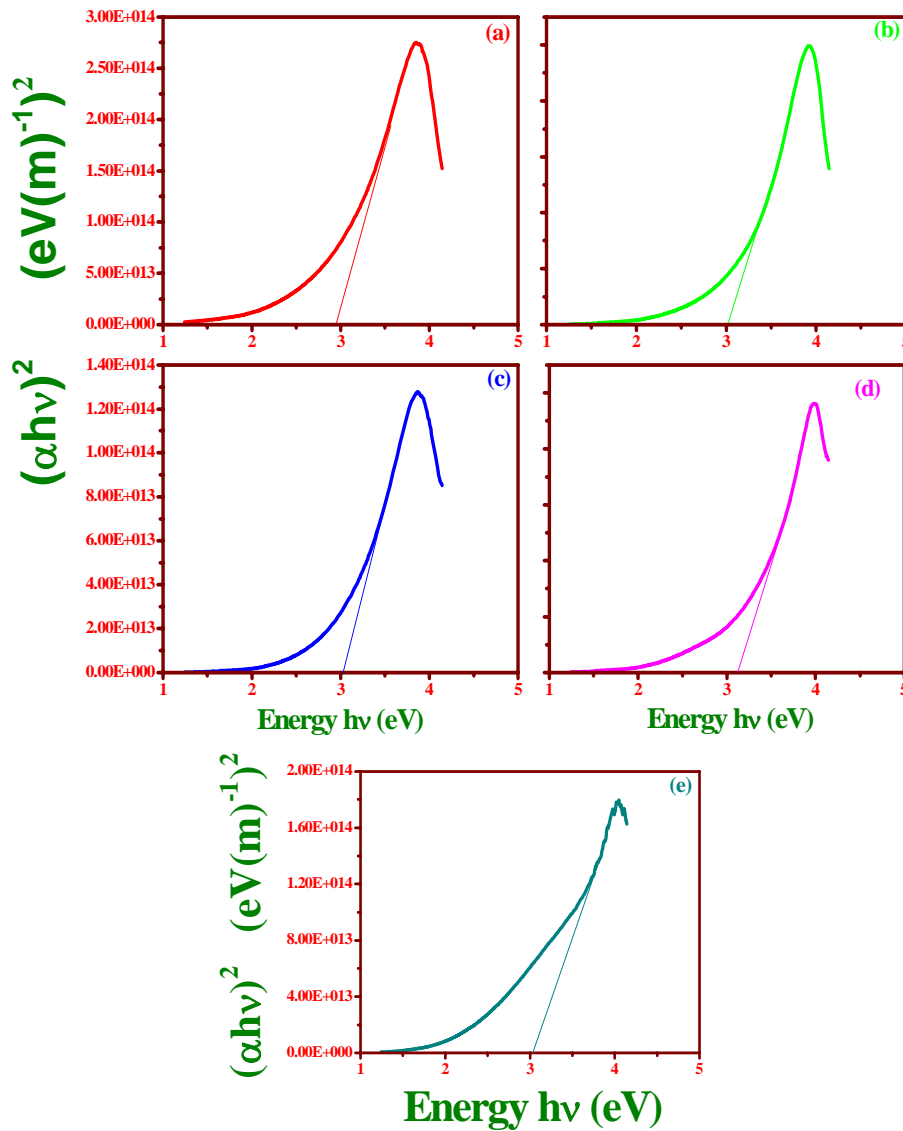


Figure 5 Variation of $(\alpha h\nu)^2$ of the ZnO (a)2 layer (b)4 layer (c)6 layer (d)8 layer (e)10 layer multilayer thin films as a function of photon energy ($h\nu$)

Photoluminescence

The PL spectra of the ZnO films exhibited UV emission peak around 383 nm, green-yellow luminescence at 496 nm. The first peak (near band edge-NBE) due to UV emissions is attributed to band-to-band transitions, excitonic emissions, and donor-acceptor pair transitions. The green-yellow band at around 496 nm is due to the deep level emissions (DLE) in green region, which is attributed to oxygen vacancies, zinc interstitials or zinc vacancies [15]. These two peaks are the most commonly found luminescent peaks in all the ZnO samples. In addition to these peaks one shoulder peak near the NBE, two shoulder peaks near DLE are also appeared. The intensities of the excitonic emissions and defects emissions decreases with increase the number of the layers and the shoulder peaks disappear for 8 and 10 layers. When the ZnO film is relatively thin, its structural disorder is relatively large and some interstitial Zn atoms exist, which possibly lead to the blue emission. With the increase of film thickness, the structural disorder decreases and the density of Zn interstitial defect is reduced. As a result, the blue emission is also decreased.

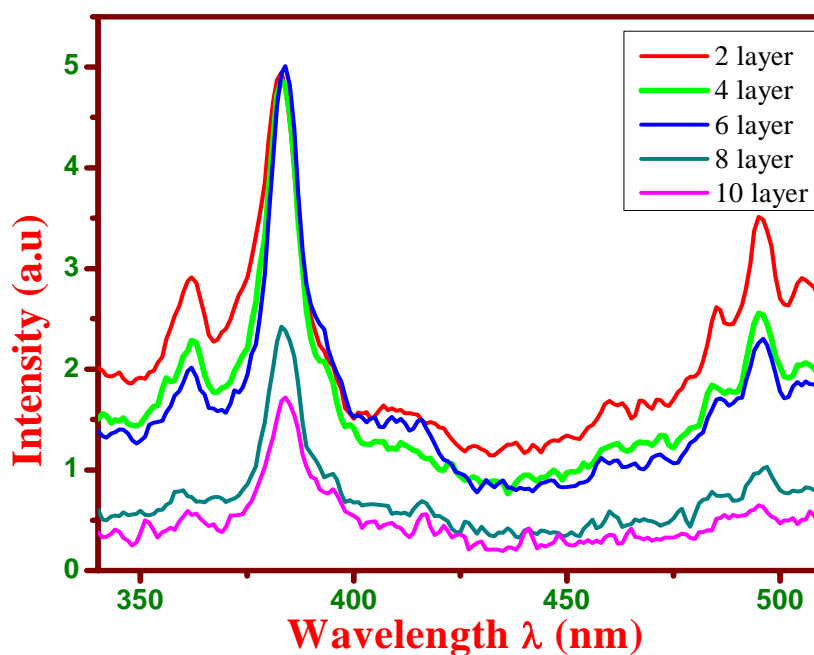


Figure 6. Room-temperature photoluminescence spectra of the samples.

Magnetic properties

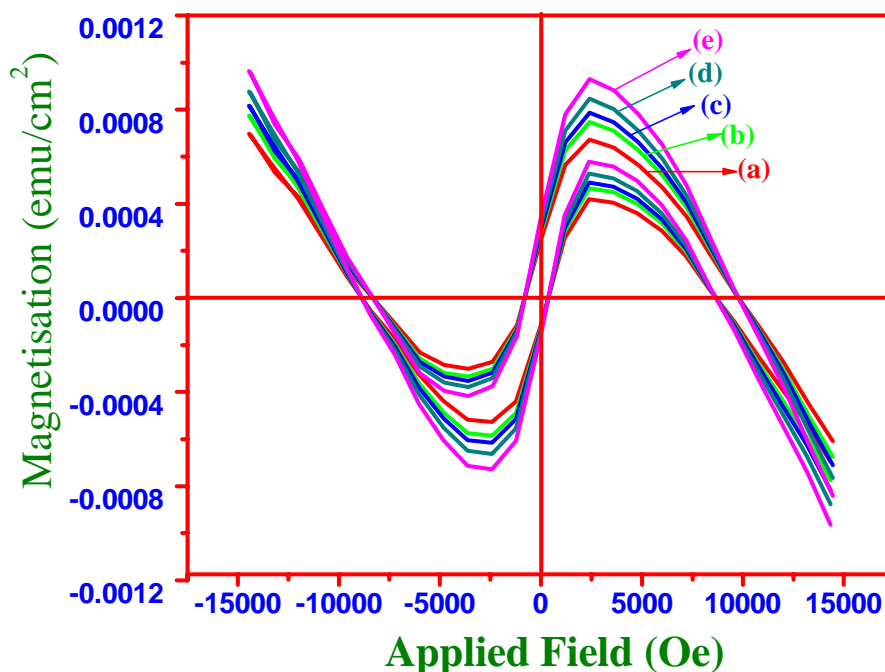


Figure 7: Magnetic hysteresis loops of Pure ZnO thin films of various thickness at room temperature.

The samples were prepared and handled carefully to avoid any possible magnetic contamination. The undoped ZnO films prepared were examined at room temperature (RT) in the range of the magnetic field 0–17.5 kOe using a Vibrating Sample Magnetometer and showed non ferromagnetic behavior, confirming that there is no extrinsic magnetic impurity contamination during the procedure of preparation. Fig. 5 presents the magnetization (M) vs magnetic field (H) of pure ZnO thin films with various thicknesses. Hysteresis curves are obtained at room temperature, showing all pure samples have non ferromagnetic characteristic. A typical diamagnetic behaviour has been observed in the bare ZnO samples. The diamagnetic behavior of pure ZnO is due to the unpaired electrons of its d orbital, which is responsible for the absence of a permanent magnetic moment.

Conclusions

In this paper we have shown that it is possible to grow ZnO thin films possessing good optical and structural properties by the solgel spin coating technique. From the XRD patterns of undoped ZnO thin films with various thickness, where all samples show similar diffraction peak positions. No peaks were observed as phases of

impurities, indicating high purity of the ZnO thin film obtained by the solgel technique. The experimental results showed that both the ultraviolet emission in PL spectrum and the magnetic properties are evidently influenced by the thickness of the film. The presence of sharp UV emission line as well as the LO-phonon lines indicates that these films have good crystalline quality. Higher thickness drastically changes the photoluminescence of spectra and shoulder peak disappears.

References

- [1] J. Wienke, B. Van der Zanden, X. Tijssen, M. Zeman, *Sol. Energy Mater. Sol. Cells* 92 (2008) 884.
- [2] C.L. Jia, K.M.Wang, X.L. Wang, X.J. Zhang, *Opt. Expr.* 13 (2005) 5093.
- [3] Sumetha Suwanboon¹, Ratana Tanattha and Ratana Tanakorn, *Songklanakarin, J.Sci. Technol.* 30 (1), 65-69, Jan. - Feb. 2008.
- [4] J.W. Xu, H. Wang, M. H. Jiang and X. Y. Liu, *Bull. Mater. Sci.*, Vol. 33, No. 2, April 2010, pp. 119–122.
- [5] Czternastek, A Brudnik, M Jachimowski and E Koiawa, *J. Phys. D: Appl. Phys.* 25 (1992) 865-870.
- [6] G. S. Tompa, S. Sun, L. G. Provost, Dan Mentel, D. Sugrim, Philip Chan, Keny Tong, Raymond Wong, and A. Lee, *Mater. Res. Soc. Symp. Proc.* Vol. 957 © 2007.
- [7] Alexandre Pourret, Philippe Guyot-Sionnest, and Jeffrey W. Elam, *Adv. Mater.* 2008, 20, 1– 4.
- [8] Tatjana Dedova , Olga Volobujeva , Jelena Klauson , Arvo Mere , Malle Krunks, *Nanoscale Res Lett* (2007) 2:391–396.
- [9] H. H. Afify, S. H. EL-Hefnawi, A. Y. Eliwa, M. M. Abdel-Naby and N. M. Ahmed, *Egypt. J. Solids*, Vol. (28), No. (2), (2005)243-254.
- [10] Dewei Chu, Yoshitake Masuda, Kazumi Kato, and Takahiro Hamada, *Phys. Status Solidi A* 206, No. 11, (2009) 2551–2554.
- [11] Mukes Kapilashrami, Jun Xu, K.V. Rao, Lyubov Belova, *Processing and Application of Ceramics* 4 [3] (2010) 225–229.
- [12] Linhua Xu, Xiangyin Li , Yulin Chen, Fei Xu, *Applied Surface Science* 257 (2011) 4031– 4037.
- [13] S. Mondal, K. P. Kanta and P. Mitra, *Journal of Physical Sciences*, Vol. 12, (2008) 221- 229.
- [14] Bin-Zhong Dong and Guo-Jia Fang, *Journal of applied physics* 101, 033713 (2007) 1-7.
- [15] Haiping Tang, Zhizhen Ye, Haiping He, *Optical Materials* 30 (2008) 1422–1426.
- [16] R.Vidya Sagar, S. Buddhudu, *Spectrochimica Acta Part A* 75 (2010) 1218–1222.